

Non-sequential double ionization of Ar: from the single- to the many-cycle regime

This content has been downloaded from IOPscience. Please scroll down to see the full text.

2014 New J. Phys. 16 033008

(<http://iopscience.iop.org/1367-2630/16/3/033008>)

View [the table of contents for this issue](#), or go to the [journal homepage](#) for more

Download details:

IP Address: 141.14.132.32

This content was downloaded on 06/05/2014 at 13:45

Please note that [terms and conditions apply](#).

Non-sequential double ionization of Ar: from the single- to the many-cycle regime

M Kübel^{1,2}, K J Betsch^{1,3}, Nora G Kling^{1,3}, A S Alnaser^{1,4,5}, J Schmidt²,
U Kleineberg², Y Deng⁶, I Ben-Itzhak³, G G Paulus^{7,8}, T Pfeifer⁹, J Ullrich^{9,10},
R Moshhammer⁹, M F Kling^{1,2,3} and B Bergues¹

¹ Max-Planck-Institut für Quantenoptik, D-85748 Garching, Germany

² Department für Physik, Ludwig-Maximilians-Universität, D-85748 Garching, Germany

³ J R Macdonald Laboratory, Physics Department, Kansas State University, Manhattan, KS 66506, USA

⁴ Physics Department, American University of Shariyah, PO Box 26666, Shariyah, UAE

⁵ Physics and Astronomy Department, King-Saud University, Riyadh 11451, Saudi Arabia

⁶ Fritz-Haber-Institut der Max-Planck-Gesellschaft, D-14195 Berlin, Germany

⁷ Institut für Optik und Quantenelektronik, Friedrich-Schiller-Universität, D-07743 Jena, Germany

⁸ Helmholtz Institut Jena, D-07743 Jena, Germany

⁹ Max-Planck-Institut für Kernphysik, D-69117 Heidelberg, Germany

¹⁰ Physikalisch-Technische Bundesanstalt, D-38116 Braunschweig, Germany

E-mail: boris.bergues@mpq.mpg.de

Received 21 October 2013, revised 19 December 2013

Accepted for publication 19 December 2013

Published 5 March 2014

New Journal of Physics **16** (2014) 033008

doi:[10.1088/1367-2630/16/3/033008](https://doi.org/10.1088/1367-2630/16/3/033008)

Abstract

The transition from the near-single to the multi-cycle regime in non-sequential double ionization of argon is investigated experimentally. Argon atoms are exposed to intense laser pulses with a center wavelength around 790 nm and the momenta of electrons and ions generated in the double ionization process are measured in coincidence using a reaction microscope. The duration of the near transform-limited pulses is varied from 4 to 30 fs. We observe an abrupt collapse of the cross-shaped two-electron momentum distribution [17] in the few-cycle regime. The transition to longer pulses is further accompanied by a strong increase in the fraction of anti-correlated to correlated electrons.



Content from this work may be used under the terms of the [Creative Commons Attribution 3.0 licence](https://creativecommons.org/licenses/by/3.0/). Any further distribution of this work must maintain attribution to the author(s) and the title of the work, journal citation and DOI.

Keywords: non-sequential double ionization, coincidence spectroscopy, strong field physics

Non-sequential double ionization (NSDI) is characterized by the correlated emission of two electrons from an atom or molecule in a strong laser field. This phenomenon, which cannot be explained within the framework of the single-active-electron approximation, was discovered more than 30 years ago [1, 2], when a knee-shaped enhancement was observed in the intensity dependent yield curve of doubly charged ions. Since then, NSDI has been the subject of numerous studies (for recent reviews see e.g. [3, 4]). In particular, it was suggested that NSDI is a manifestation of the rescattering process [5, 6]. The observation of the characteristic double hump structure in the recoil-ion momentum spectra of doubly and multiply charged ions provided clear evidence that the emission of the second electron is triggered by the laser-driven recollision of the first electron with its parent ion [7].

A deeper insight into the NSDI process was provided by kinematically complete experiments where the correlated two-electron momentum distributions (briefly, two-electron spectrum) were measured. In particular, such measurements permit one to distinguish between (positively) correlated [8] and anti-correlated [9] electron emission, as illustrated in figure 1.

Correlated electron emission, in which the two electrons are ejected in the same direction (i.e., equal sign momenta), is usually attributed to direct electron impact ionization [10]. Anti-correlated electron emission, where the two electrons are ejected in opposite directions (i.e., opposite sign momenta), is ascribed to recollisional excitation and subsequent ionization [9]. Further studies revealed that the fraction of anti-correlated electrons to the total yield increases with decreasing laser intensity [11] and can even dominate at low intensity [12]. Classical-ensemble calculations [13] suggest that multiple recollisions of the electron with the parent core play a major role in the production of anti-correlated electrons [12].

Owing to the great advances in ultra-fast laser technology [14, 15], two-electron spectra could recently be measured using few-cycle [16] and near-single-cycle [17] pulses with known carrier-envelope phase (CEP). This has allowed the study of NSDI of Ar and N₂ in the extreme limit of a single recollision event [17, 18]. When averaged over CEP, the two-electron spectra were found to exhibit a cross-like shape. This feature, which is distinctively different from all previous experimental results obtained with longer pulses could be well reproduced by a semi-classical model based on recollision excitation with sub-cycle depletion [17].

The goal of the present study is to investigate the transition from single- to multi-cycle NSDI by recording correlated two-electron momentum distributions for laser-pulse durations ranging from 4 to 30 fs. We demonstrate that for a fixed intensity, the characteristic cross-shaped structure observed for 4 fs near Fourier-transform-limited pulses [17] quickly changes when the pulse duration is increased. This is accompanied by a rise in the yield ratio of anti-correlated to correlated electrons and associated with significant changes in the single-ionization dynamics.

The experimental setup has been outlined previously [17, 19]. Briefly, linearly polarized laser pulses with a central wavelength of 790 nm are generated at a repetition rate of 10 kHz in a chirped-pulse amplification (CPA) Ti:Sapphire laser-system and focused into a hollow-core fiber for spectral broadening. The laser pulse duration is varied by clipping the edges of the spectrum in the prism compressor of the CPA-laser system and adjusting the gas pressure in the hollow-core fiber. After the fiber, the pulses are compressed to near-Fourier-limited pulses using

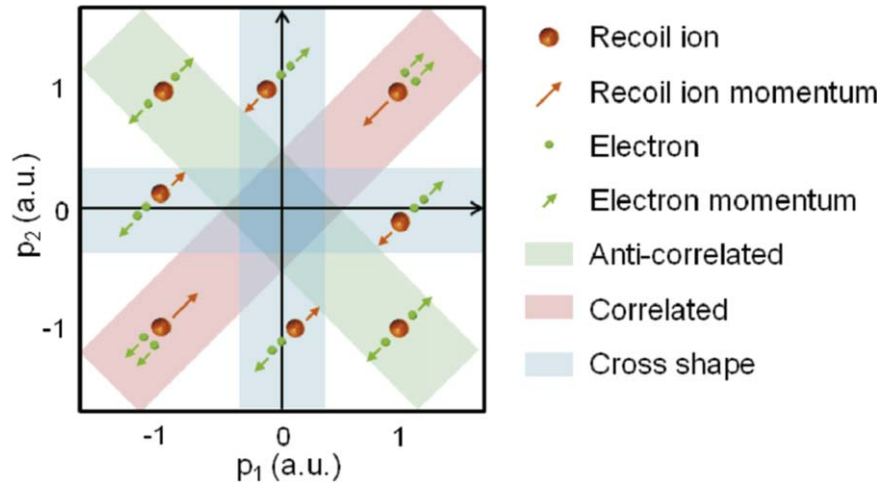


Figure 1. Illustration of the momentum sharing between the two electrons (green spheres) and the ion (orange sphere) after double ionization. Events in the red area in the first and third quadrants correspond to correlated electron emission (i.e. the momentum vectors of the two electrons point to the same direction). Events in the green area in the second and fourth quadrants correspond to anti-correlated electrons emission (i.e. the momentum vectors of the two electrons point to opposing directions). The blue cross-shaped area corresponds to events with totally asymmetric kinetic-energy sharing of the electrons along the laser polarization direction (i.e. one of the two electrons carries most of the kinetic energy).

chirped mirrors and fused silica wedges. The pulse duration is measured by fringe-resolved autocorrelation. The retrieved pulse durations are found to agree with those of the Fourier-limited pulses calculated from the measured laser spectra, suggesting a minimal chirp. We estimate the accuracy of the pulse-duration measurement to be on the order of 15%. The laser pulses are focused into a cold supersonic argon jet inside a reaction microscope (REMI) [20] in which the momenta of ions and electrons generated in the laser focus are measured in coincidence. The peak intensity is controlled using an iris aperture at the entrance of the REMI. Its value of about $1.0 \times 10^{14} \text{ W cm}^{-2}$ is estimated from the $10 U_p$ cut-off of the simultaneously measured single-ionization photoelectron spectra of Ar.

The two-electron spectra are generated by selecting all events in which at least one electron and one Ar^{2+} ion were detected. The second electron momentum is calculated as the negative momentum sum of the detected ion and the first electron. In order to reduce the effect of false coincidences, only events with a positive Ar^{2+} momentum (i.e. a momentum directed towards the ion detector) are considered. The total number of events in a two-electron spectrum is typically of the order of 10 000 and the estimated fraction of false coincidences to the total signal is smaller than 7%. The two-electron spectra are symmetrized with respect to the $p_2 = -p_1$ diagonal. Because the first and second electron are experimentally not distinguishable, the signal is also symmetrized with respect to the $p_2 = p_1$ diagonal.

In figure 2(a) we show the distributions of momenta p_{\parallel} of Ar^+ and Ar^{2+} that were recorded for pulse durations of 4, 8, 16 and 30 fs (p_{\parallel} denotes the momentum component parallel to the laser polarization direction). The widths of the Ar^+ spectra match fairly well, indicating that the peak intensity values for the different pulse durations were kept constant within an accuracy of

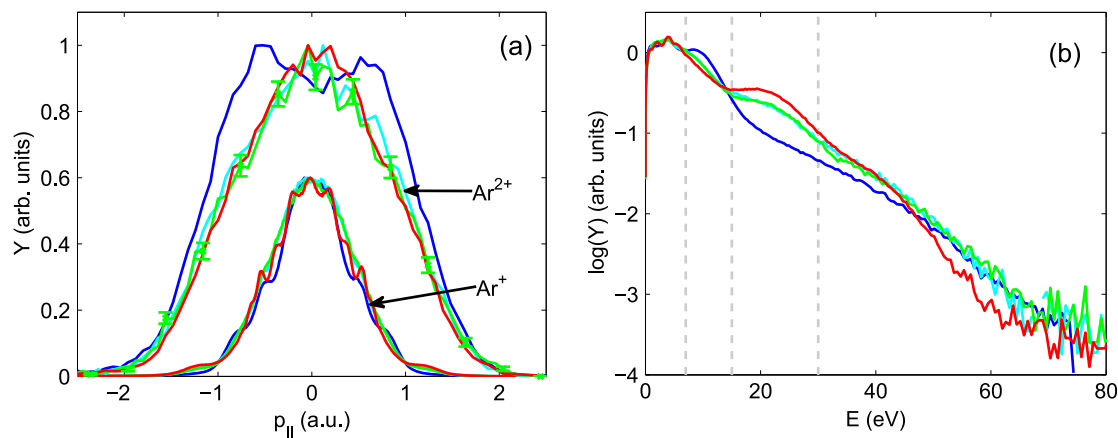


Figure 2. (a) Measured recoil-momentum distributions of Ar^+ and Ar^{2+} ions generated by 4 fs (blue), 8 fs (cyan), 16 fs (green), and 30 fs (red) pulses at a peak intensity of $1.0 \times 10^{14} \text{ W cm}^{-2}$. For visual convenience the maxima of the momentum distributions of Ar^{2+} and Ar^+ are normalized to 1 and 0.6, respectively. Representative statistical error bars are shown for the Ar^{2+} signal generated with a 16 fs pulse. For the Ar^+ signal, the statistical error bars are on the order of the line thickness. (b) Single-ionization photoelectron energy spectra obtained via momentum conservation from the Ar^+ momentum distributions shown in (a). Each curve is normalized to its integral and the color coding is the same as in (a). The gray dashed lines mark the energy ranges $E = 7\text{--}12 \text{ eV}$, and $E = 12\text{--}30 \text{ eV}$, in which the pulse-duration dependence is most pronounced.

15%. Despite their similar widths, the Ar^+ spectra exhibit different features for different pulse durations. While the spectra are rather smooth for the intermediate pulse durations (8 and 16 fs), clear modulations originating from intra-cycle interferences [21–23] are visible for 4 fs and inter-cycle interferences resulting in the above threshold ionization (ATI) peaks can be seen at 30 fs. Due to the limited ion momentum resolution of about 0.1 au, the ATI peaks can only be resolved at low momenta where they are spaced sufficiently apart.

The single ionization photoelectron spectra shown in figure 2(b) exhibit a strong pulse-duration dependence in the energy range between 7 and 30 eV. In the region between 7 and 12 eV, the drop of the signal with increasing energy is considerably faster for longer pulses than for short ones. In the low-energy plateau region (from 15 to 30 eV), in contrast, the situation is reversed, giving rise to the ATI-enhancement reported in [24]. Quantum mechanical models [25], as well as semi-classical considerations [26] invoke multiple recollisions to explain this feature and its pulse duration dependence [28]. Its absence in the near single-cycle regime, for which multiple recollisions are fully suppressed, provides further evidence for the essential role of the latter in the build-up of the ATI enhancement.

As can be seen in figure 2(a), the shapes of the Ar^{2+} spectra generated with multi-cycle pulses (8, 16 and 30 fs) do not significantly differ from each other. They exhibit a maximum at zero momentum, in contrast to the Ar^{2+} spectrum generated with a 4 fs pulse, which exhibits a pronounced dip around $p_{||} = 0$. This is consistent with previous observations by Rudenko *et al* [27] who reported the appearance of a similar dip when decreasing the pulse duration from 25 to 7 fs.

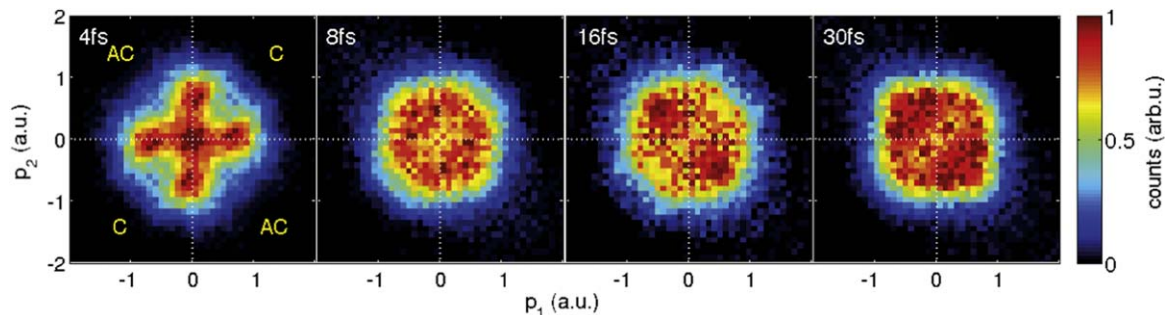


Figure 3. CEP-averaged two-electron spectra emerging from NSDI of Ar for different laser pulse durations at a peak intensity of $1.0 \times 10^{14} \text{ W cm}^{-2}$ as indicated in the figures. p_1 and p_2 denote the photoelectron momenta along the laser polarization. Invariance with respect to the $p_2 = p_1$ and $p_2 = -p_1$ diagonals were used to symmetrize the spectra. The labels C and AC in the first panel denote the quadrants with correlated and anti-correlated electron emission, respectively.

A more detailed understanding of the sudden change in the NSDI dynamics accompanying the transition into the few-cycle regime can be gained from the measured two-electron spectra. As shown in figure 3, the shapes of the two-electron spectra for 4 and 8 fs are qualitatively different. Starting from a cross shape for near-single-cycle pulses, the signal is more homogeneously distributed over the four quadrants of the two-electron spectrum for the longer pulse durations. At first sight, the 8 fs results are reminiscent of the uncorrelated momentum distribution that is expected for sequential double ionization [8]. Although the rate of sequential ionization increases with the pulse duration, such a rapid transition from NSDI to sequential ionization would be rather astonishing. As a matter of fact, a significant contribution of sequential double ionization can be ruled out for the following reasons: (i) the yield ratio of Ar^{2+} and Ar^+ was less than 0.3% in all measurements presented in figure 3. Comparison of this ratio with the results of previous studies [29] indicates that the intensity used in our experiment was too low for the sequential ionization mechanism to dominate double ionization. (ii) As will be shown in figure 5, two-electron spectra recorded at higher intensity exhibit predominantly positively correlated electron momenta. This finding, which is consistent with the results of previous studies performed in the many-cycle regime (see for instance [8]), yields further evidence that the data shown in figure 3 were recorded at intensities well below the onset of sequential ionization. For a pulse duration of 8 fs, NSDI thus results in approximately equal contributions of positively correlated and anti-correlated electron emission.

With increasing pulse duration, however, significant deviations from an uncorrelated momentum distribution can be identified. Between 8 and 30 fs, the two-electron spectra exhibit a clear trend towards increasing anti-correlated electron emission. For two-electron spectra recorded at 16 and 30 fs the signal of anti-correlated electrons is stronger and extends to slightly higher momenta as compared to the result obtained with 8 fs pulses. The magnitude of the enhancement of anti-correlated electron emission with increasing pulse duration is quantified by plotting the ratio N_{AC}/N_C in figure 4. Here, N_C (N_{AC}) is the integrated signal in the first ($p_1, p_2 > 0$) and third ($-p_1, -p_2 > 0$) (second ($-p_1, p_2 > 0$) and fourth ($p_1, -p_2 > 0$)) quadrants. It can be seen that the relative contribution of anti-correlated electron emission tends to saturate for $\tau \gtrsim 8$ fs. This suggests that the observed transition in the NSDI dynamics originates from

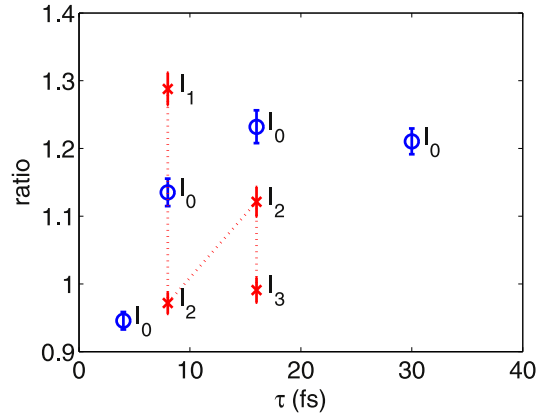


Figure 4. Dependence of the yield ratio of anti-correlated to correlated electrons N_{AC}/N_C on the pulse duration. The error bars include both statistical uncertainty and systematic errors due to false coincidences. Data points with blue circles and red crosses are obtained from the two-electron spectra of figures 3 and 5, respectively. The dotted red line serves as a guide to the order in which the data points are described in the text.

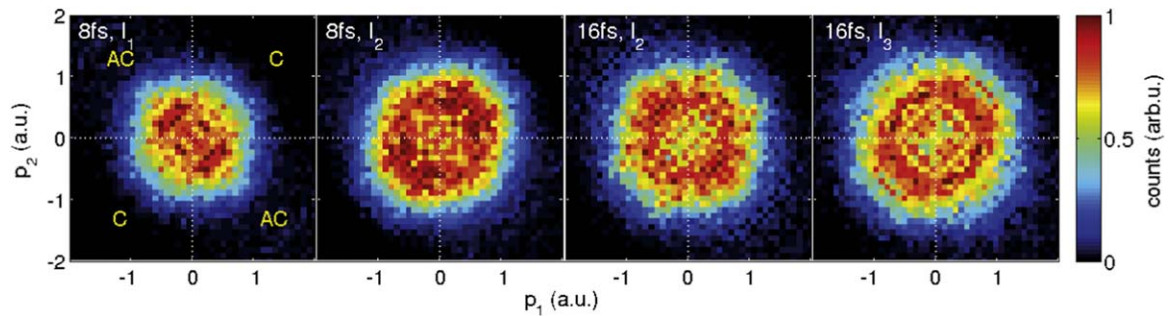


Figure 5. Two-electron spectra for NSDI of Ar recorded at different intensities $I_1 = 0.8 \times 10^{14} \text{ W cm}^{-2}$, $I_2 = 1.2 \times 10^{14} \text{ W cm}^{-2}$, $I_3 = 1.4 \times 10^{14} \text{ W cm}^{-2}$ and pulse durations as indicated in the figure.

the contribution of only a small number of additional recollisions, confirming the exponential decay of the recollision probability described in [30].

In order to discuss the combined effect of intensity and pulse duration on NSDI, let us turn to the experimental results displayed in figure 5. The two-electron spectrum shown in the first panel was recorded at an intensity of $I_1 = 0.8 \times 10^{14} \text{ W cm}^{-2}$ and for a pulse duration of 8 fs. For these laser parameters the emission of anti-correlated electrons is slightly favored. Increasing the intensity to $I_2 = 1.2 \times 10^{14} \text{ W cm}^{-2}$, while keeping the pulse duration fixed, results in the two-electron spectrum shown in the second panel, for which correlated electron emission is preferred. As shown in the third panel, this trend can be reversed simply by increasing the pulse duration to 16 fs while the intensity is kept constant. In the fourth panel the intensity is increased to $I_3 = 1.4 \times 10^{14} \text{ W cm}^{-2}$ while the pulse duration is kept constant at 16 fs. Thereby some of the preferred emission of correlated electrons is recovered. The observed trends are quantified by plotting the yield ratio of correlated to anti-correlated electrons as red data points in figure 4. In summary, the above results support the following

conclusions: (i) increasing the pulse duration enhances anti-correlated electron emission and (ii) the observations that positively correlated electron emission increases with intensity [11, 12], is also valid in the few-cycle regime.

While the semi-classical model for recollision excitation with sub-cycle depletion [17, 18] performs well in the limiting case of single-cycle NSDI, an extension of this model to the case of multiple recollisions is demanding because of the large number of additional ad hoc assumptions required. Besides the more exact but also more challenging quantum mechanical computations [31–33], classical ensemble calculations [13, 34, 35] have proven to be a pragmatic and successful alternative route to describe NSDI. While they naturally account for multiple recollisions that lead to a repeated energy exchange between the electrons and the ionic core, these models could also explain the emission of anti-correlated electrons in longer pulses [36]. Very recently, Huang *et al* [37] were able to accurately describe our recent single-cycle NSDI experiment [17] using a classical ensemble model, suggesting that simulating the experimental results of the present study should be within reach.

In conclusion, we have investigated NSDI of Ar in the transition from the near-single-cycle to the many-cycle regime. We found that the main change in the dynamics occurs abruptly between 4 and 8 fs. In particular, the contribution of anti-correlated electron emission to NSDI strongly increases from 4 to 8 fs and tends to saturate soon beyond 8 fs, which suggests that only a few recollisions efficiently contribute to NSDI. Our results demonstrate that besides the peak intensity, the pulse duration provides a sensitive knob to control anti-correlated electron emission. More importantly, our data provide a solid basis for assessing the validity of different theoretical approaches and will hopefully contribute to the emergence of a coherent and quantitative theoretical description of NSDI from the single to the multi-cycle regime.

Acknowledgments

We appreciate fruitful discussions with Artem Rudenko. We thank Ferenc Krausz for his support and for making specialized equipment available to us. BB acknowledges additional support from Laszlo Veisz and ASA acknowledges support from the American University of Sharjah-UAE. We are grateful for support from the Max-Planck Society and the DFG via grants KI-1439/3, KI-1439/5 and the Cluster of Excellence: Munich Center for Advanced Photonics (MAP). JRML personnel acknowledges support from the Chemical Sciences, Geosciences, and Biosciences Division, Office of Basic Energy Sciences, Office of Science, US Department of Energy.

References

- [1] Suran V V and Zapesochnyi I P 1975 *Sov. Tech. Phys. Lett.* **1** 420
- [2] L’Huillier A, Lompré L A, Mainfray G and Manus C 1982 *Phys. Rev. Lett.* **48** 1814
- [3] Figueira de Morisson F C and Liu X 2011 *J. Mod. Opt.* **58** 1076
- [4] Becker W 2012 *Rev. Mod. Phys.* **84** 1011
- [5] Krause J L, Schafer K J and Kulander K C 1992 *Phys. Rev. Lett.* **68** 3535
- [6] Corkum P B 1993 *Phys. Rev. Lett.* **71** 1994
- [7] Moshhammer R *et al* 2000 *Phys. Rev. Lett.* **84** 447
- [8] Weber Th *et al* 2000 *Nature* **405** 658

- [9] Feuerstein B *et al* 2001 *Phys. Rev. Lett.* **87** 043003
- [10] Kopold R, Becker W, Rottke H and Sandner W 2000 *Phys. Rev. Lett.* **85** 3781
- [11] de Jesus V L B *et al* 2004 *J. Phys. B: At. Mol. Opt. Phys.* **37** L161
- [12] Liu X *et al* 2008 *Phys. Rev. Lett.* **93** 263001
- [13] Ho P J *et al* 2005 *Phys. Rev. Lett.* **94** 093002
- [14] Hentschel M *et al* 2001 *Nature* **414** 509
- [15] Baltuška A *et al* 2003 *Nature* **421** 611
- [16] Camus N *et al* 2012 *Phys. Rev. Lett.* **108** 073003
- [17] Bergues B *et al* 2012 *Nat. Commun.* **3** 813
- [18] Kübel M *et al* 2013 *Phys. Rev. A* **88** 023418
- [19] Johnson N G *et al* 2011 *Phys. Rev. A* **83** 013412
- [20] Ullrich J *et al* 2003 *Rep. Prog. Phys.* **66** 1463
- [21] Bergues B *et al* 2007 *Phys. Rev. A* **75** 063415
- [22] Arbó D G *et al* 2010 *Phys. Rev. A* **81** 021403
- [23] Gopal R *et al* 2009 *Phys. Rev. Lett.* **103** 053001
- [24] Hertlein M P 1997 *J. Phys. B* **30** L197
- [25] Muller H G and Kooiman F C 1998 *Phys. Rev. Lett.* **81** 1207
- [26] Paulus G G *et al* 2001 *Phys. Rev. A* **64** 021401R
- [27] Rudenko A *et al* 2004 *Phys. Rev. Lett.* **93** 253001
- [28] Grasbon F *et al* 2004 *Phys. Rev. Lett.* **91** 173003
- [29] Guo C *et al* 1998 *Phys. Rev. A* **58** R4271
- [30] Ho Phay and Eberly J 2005 *Phys. Rev. Lett.* **95** 193002
- [31] Shaaran T, Nygren M T and Figueira de Morisson F C 2010 *Phys. Rev. A* **81** 063413
- [32] Parker J S *et al* 2006 *Phys. Rev. Lett.* **96** 133001
- [33] Ruiz C *et al* 2006 *Phys. Rev. Lett.* **96** 053001
- [34] Mauger F *et al* 2012 *Phys. Rev. Lett.* **108** 063001
- [35] Emmanouilidou A and Staudte A 2009 *Phys. Rev. A* **80** 053415
- [36] Haan S L, Smith Z S, Shomsky K N and Plantinga P W 2008 *J. Phys. B: At. Mol. Opt. Phys.* **41** 211002
- [37] Huang C *et al* 2013 *Opt. Express* **21** 11382